Microelectronic Engineering 162 (2016) 1–5

Contents lists available at ScienceDirect

Microelectronic Engineering

journal homepage: www.elsevier.com/locate/mee

Research paper

Fractal cross aperture nano-antenna with graphene coat for bio-sensing application

Mohammad Nasser Moghadasi [a], Ramazan Ali Sadeghzadeh [b], Mohammad Toolabi [a], Payam Jahangiri [a], Ferdows B. Zarrabi [c,*]

[a] Department of Electrical and Computer Engineering, Science and Research Branch, Islamic Azad University, Tehran, Iran
[b] Faculty of Electrical Engineering, K.N. Toosi, University of Technology, Tehran, Iran
[c] Young Researchers and Elite Club, Babol Branch, Islamic Azad University, Babol, Iran

ARTICLE INFO

Article history:
Received 29 December 2015
Received in revised form 22 March 2016
Accepted 24 April 2016
Available online 26 April 2016

Keywords:
Nano-aperture
Graphene
Bio-sensing
High Q-factor
Fractal

ABSTRACT

In this paper, we presented a novel shape for nano-aperture for biomedical and spectroscopy application. In addition, when the graphene coat layer is added to structure, we are achieving a reconfigurable particle with more transmittance and the impedance parameters can describe the effect of the graphene layer. The prototype structure is simulated with the FDTD method by the CST microwave studio and for the substrate, the SiN layer with refractive index of 1.98 and thickness of 80 nm is selected. The Palik model is implemented for the gold layer with thickness of 30 nm, and single graphene layer is selected for a coat with 1 nm thickness. The prototype antenna has the dual band characteristic at 46 and 86 THz for biomedical sensing at mid infrared application. The graphene coat is improving the transmittance in the prototype nano-particle. Here we show that the graphene layer implementation is useful for making biosensor with more accuracy and sensitivity. The prototype structure shows orthogonal characteristic that made it useful for solar cell application and energy harvesting in by enhancement of electrical field in both X and Y directions.

1. Introduction

Nowadays, developments of micro and nano technology at THz and optical regime are resulted many new devices at THz or optical sensors for detection of small partial such as biological and chemical materials that are important in medicine, genetic analysis and the pharmaceutical and food industries [1–2].

Surface plasmon polaritons (SPPs) are indicated of the electromagnetic excitations with the metal-dielectric layer and are appearing at the interface between dielectric and metallic layers, and SPPs are used for different application such as field enhancement [3], subwavelength propagation [4], subwavelength waveguide [5], molecule detection [6], surface Raman scatters enhancement [7] and near-field coupling effects [8].

Various shapes of the aperture nano-antenna are studied by Altug et al. for the spectroscopy and bio-sensing for infrared domain (IR) such as an H-shape with sensitivity to polarization [9] Jerusalem cross [10] Multi-resonant Metamaterials based on UT-shaped nano-aperture [11].

Graphene is used as an optical application from THz to the optical regime for achieving reconfigurable characteristic at tunable dipole nano-antenna and absorber [12–13]. The σ_{intra} formation is used as the surface conductivity of the graphene for THz application for less than 10 THz [14] and the σ_{inter} formation is implemented for the surface conductivity of the graphene at optical application for more than 150 THz [15]. However, for the mid infrared application, the Kubo formula performances are implemented for graphene in these studies and graphene's conductivity has two various terms of the σ_{inter} and the σ_{intra} and therefore $\sigma_G(\omega) = \sigma_{inter}(\omega) + \sigma_{intra}(\omega)$ [16].

Recently, graphene has been noticed with single or multilayer structures to enhance the transmittance and the absorption cross section in nano-antenna and nano-particle [17–18].

By Altug et al. debated about the fabrication process of the nano-aperture in six photolithography steps with UV-light, dry etching by SF6 and He, wet etching by KOH, E-beam lithography with PMMA, dry etching by SF6 and Ar and at last metal deposition by using gold and Titanium for bonding of gold to SiN layer [19–20].

In addition, fractal geometry is made by mathematical abstraction of self-similar or self-off-line that are improving the radiation quality in nano particle or absorber with various formations such as a snowflake, a tree and bowtie [21].

Sierpinski fractal plasmonic nanoantennas are conventional models of fractional form for bowtie or rectangular structure as a fractal carpet in optical regime [22–23]. In addition, the fractal carpets are used in plasmonic absorber for enhancement in the surface absorption of solar cell application [24].

Furthermore, the fractal formation is noticed in nano aperture for optical imaging [25].

* Corresponding author.
E-mail address: ferdows.zarrabi@yahoo.com (F.B. Zarrabi).

http://dx.doi.org/10.1016/j.mee.2016.04.022
0167-9317/

In this article, the final modeled nano-antenna has the dual band characteristic at 46 and 86 THz, and it is implemented for biomedical sensing at mid-infrared application. We have used commercial FDTD software by using two-port analyzing for transmittance studies, and results are compared with simple cross-junction model, and we show that the prototype nano-antenna has the independence to incident polarization. Here we show that with the implementation of the fractal formation the electrical field in both X and Y directions is increased drastically and structure shows orthogonal polarization.

2. Design particles

Fig. 1(a) shows the novel cross-loop shaped nano-aperture and graphene layer over the gold layer at Fig. 1(c). The structure contains a gold layer with cross-loop shape aperture with length of 2400 nm and width of 2400 nm with a thickness of 30 nm. In Fig. 1(b) we show the fractional nano-antenna design process in 3 steps and result of these antennas is compared together. The gold layers are placed on the SiN layer with n = 1.98 that is selected as a substrate with a thickness of 80 nm and Palik's model of gold is selected for the gold parts in our structure.

CST microwave studio full wave simulator has done the simulation with time domain method and the open boundary with 300 nm distance by conventional PML (perfectly match layer) is selected. Accordingly, we are covering the gold layer with a multilayer graphene with a thickness of 1 nm as shown in Fig. 1(c).

We should have noticed that the single-layer graphene cannot bond to gold layer and therefore. For bonding of the Au with a single layer, graphene (SLG) by Electron-beam lithography a thin layer of Cr + should be deposited over the gold layer before deposition of the graphene [26]. Here, in simulation, because of little thickness [around 5 nm] of the Cr, we are neglecting the effect on our simulation. In addition, all dimensions are a = b = 2400 nm, c = 600 nm, d = 100 nm.

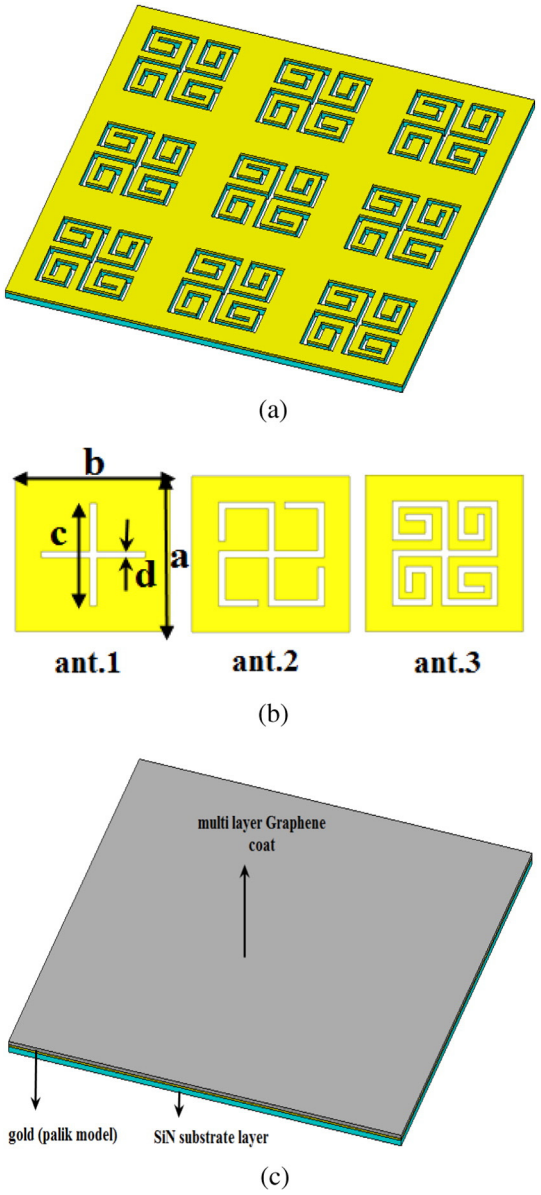

Fig. 1. The geometric of the nano-antenna (a) final prototype nano-antenna (b) three types of the designing of the nano-antenna and the dimensions are a = b = 2400 nm, c = 600 nm, d = 100 nm (c) final prototype antenna with multilayer graphene

3. Simulation result and discussions

For numerically analyze, the aperture system, we use FDTD by using two-port analyzing where the ports are placed in front of the array structure. The boundary condition is selected open for sidewalls and open with space in Z and -Z directions. The Fig. 2(a) shows the transmission of a three step of nano-antenna without the graphene layer.

In the first antenna, the nano-antenna has a resonance at 62 THz (λ = 4830 nm) and the resonance pick is about 0.63 for transmission.

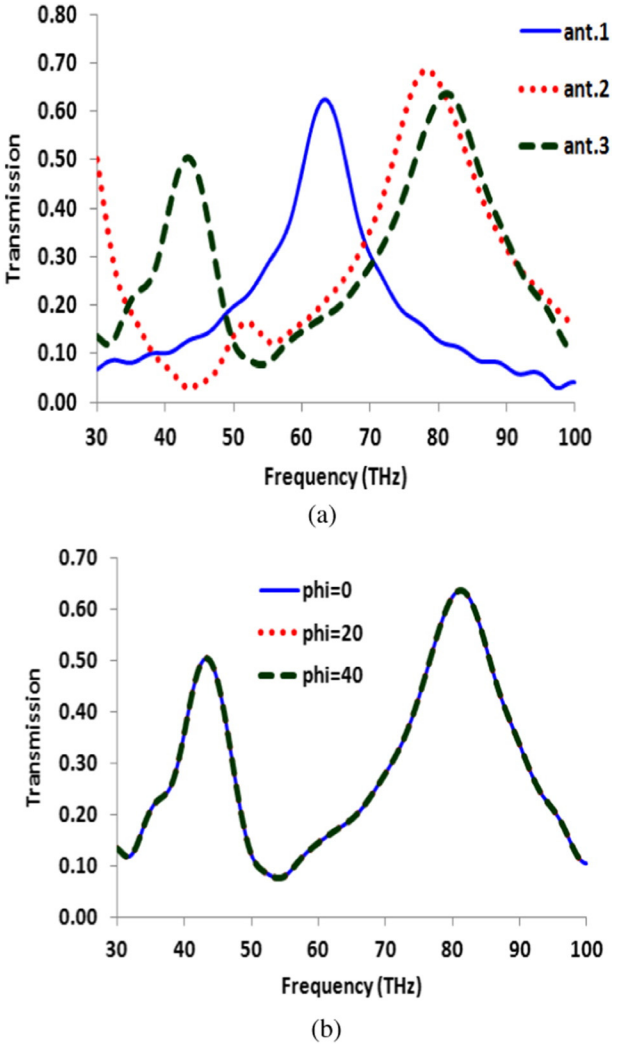

Fig. 2. The transmission of nano-antenna (a) three type of nano-antenna (b) various polarization angle for phi = 0°, 20° and 40°.

Because of the symmetrical structure that is used in this study, the effects of the polarization in y and x directions are neglected.

In the second antenna, the nano-antenna has two resonances at 30 and 80 THz ($\lambda = 9990$ nm and $\lambda = 3750$ nm) and the resonance pick is about 0.5 and 0.7 for transmission respectively.

In the final antenna, the nano-antenna has two resonances at 42 and 82 THz ($\lambda = 7137$ nm and $\lambda = 3656$ nm) and the resonance pick is about 0.5 and 0.65 for transmission respectively.

The incident wave polarization independency of the nano-aperture antenna is studied at Fig. 2(b) for phi = 0°, 20° and 40° and here, we show that the change in polarization has not any effect on the transmittance of our prototype nano-antenna and resonances are fixed at 42 and 82 THz.

Furthermore, for nano-antenna with graphene coat, we are implementing the single-layer graphene coat with thickness of 1 nm and in Fig. 3 we are studying the conductivity of the single-layer graphene manner at a range of 30–100 THz and biasing effect of on conductivity. For modeling of the graphene, the temperature and relaxation time are assumed 293[K] and 0.1[ps], respectively. As shows in here, by increasing the chemical potential in graphene the conductivity is increased and shifted to higher frequency. Therefore, by applying the graphene to the prototype antenna the surface impedance is increased in nano-particle and matching is amended, and therefore, we expected to achieve more transmittance in our final model by increasing the chemical potential in graphene layer to 0.3 eV.

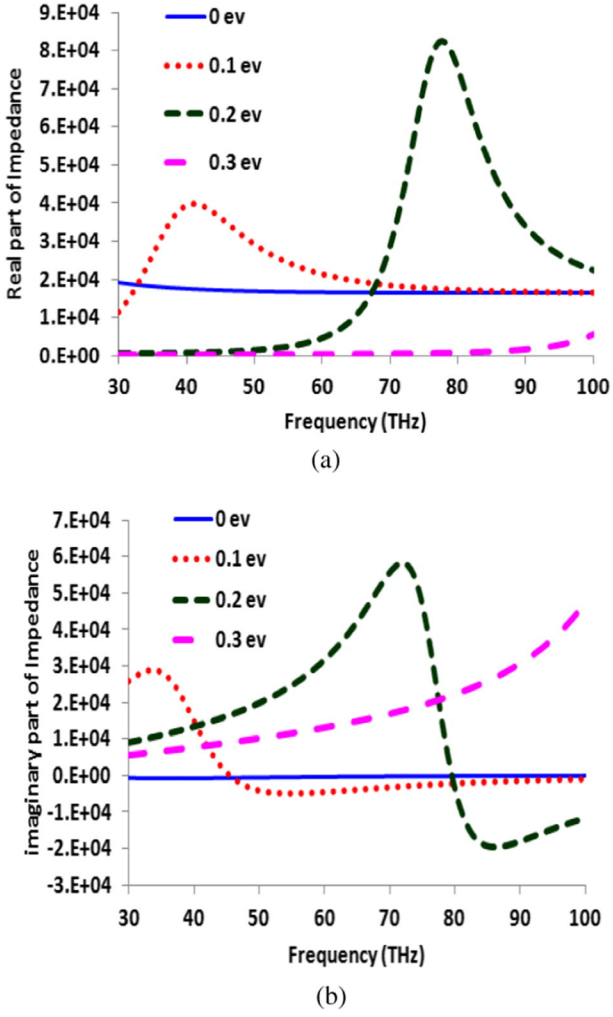

Fig. 3. The conductivity of the graphene in the range of 30–100 THz for the chemical potential in the range of 0 to 0.3 eV (a) the real part (b) the imaginary part.

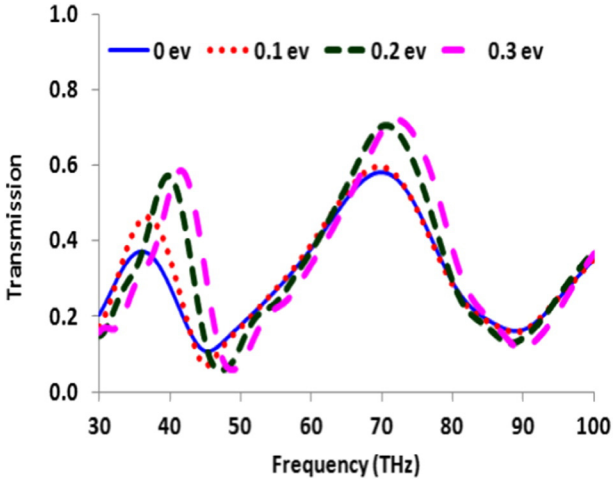

Fig. 4. The transmission of the nano-antenna with various graphene biasing.

In this step, we added the single-layer graphene to the prototype nano-aperture, and then we are biasing the graphene layer with various chemical potentials (0 to 0.3 eV) and the results of transmittance are presented at Fig. 4 for single layer graphene with a thickness of 1 nm. By biasing the graphene layer to higher voltage the frequency is shifted to higher frequency. Without biasing of the graphene, the transmittance is a decrease in prototype nano-antenna. However, by increasing the voltage of biasing the transmittance is increased to 0.62 and 0.75 respectively for first and second resonance.

Fig. 5(a) shows the electric field (E-field) intensity enhancement distribution for the simple cross structure (ant.1) and in addition, we compared the result with second (ant.2) and third model (ant.3) nano-aperture at Fig. 5(b) and (c) respectively. As shown in here the first antenna has linear polarization and second and third antenna shows the orthogonal polarization.

For the first antenna the $|E^2|/|E_{int}{}^2|$ ratio in X-direction and Y-direction are 1705 $(V/m)^2$ and 3.7 $(V/m)^2$ respectively, and total $|E^2|/|E_{int}{}^2|$ ratio 1823 $(V/m)^2$ at 64 THz.

For the second nano-antenna the $|E^2|/|E_{int}{}^2|$ ratio in X-direction and Y-direction are 610 $(V/m)^2$ and 506 $(V/m)^2$ respectively and total $|E^2|/|E_{int}{}^2|$ ratio 1169 $(V/m)^2$.

For the third antenna the $|E^2|/|E_{int}{}^2|$ ratio in X-direction and Y-direction are 784 $(V/m)^2$ and 918 $(V/m)^2$ respectively, and total $|E^2|/|E_{int}{}^2|$ ratio1866 $(V/m)^2$ at 42 THz. Its visible the new form of the cross structure help full in achieving orthogonal properties in nano-aperture and also the E-field enhancement is increase in comparison to simple cross aperture.

In the final nano-antenna, when the graphene layer with thickness of 1 nm and chemical potential of the 0.3 eV is added to final aperture model the $|E^2|/|E_{int}{}^2|$ ratio in X-direction and Y-direction are 1197 $(V/m)^2$ and 1346 $(V/m)^2$ respectively and total $|E^2|/|E_{int}{}^2|$ ratio 2724 $(V/m)^2$ at 40 THz.

For revealing the effect of bilateral on prototype nano-antenna, we choose four conventional biomaterial and here we investigated the effect on transmission and electrical field.

Surface enhanced infrared absorption (SEIRA) spectroscopy is a conventional procedure for detection of material such as Ether(R–O–R′) with n = 1.35, Ethylene glycol (HO–CH2CH2–OH) with n = 1.43, Chlorobenzene (C6H5Cl) with n = 1.525, and Quinoline (C6H7N) with n = 1.627 [27].

The transmission of the prototype nano-aperture in the presence of the additional material are presented for two various biasing (0.1 and 0.3 eV) for graphene and results are given at Fig. 6(a) and (b) respectively and bio material thickness are assumed 30 nm in this study.

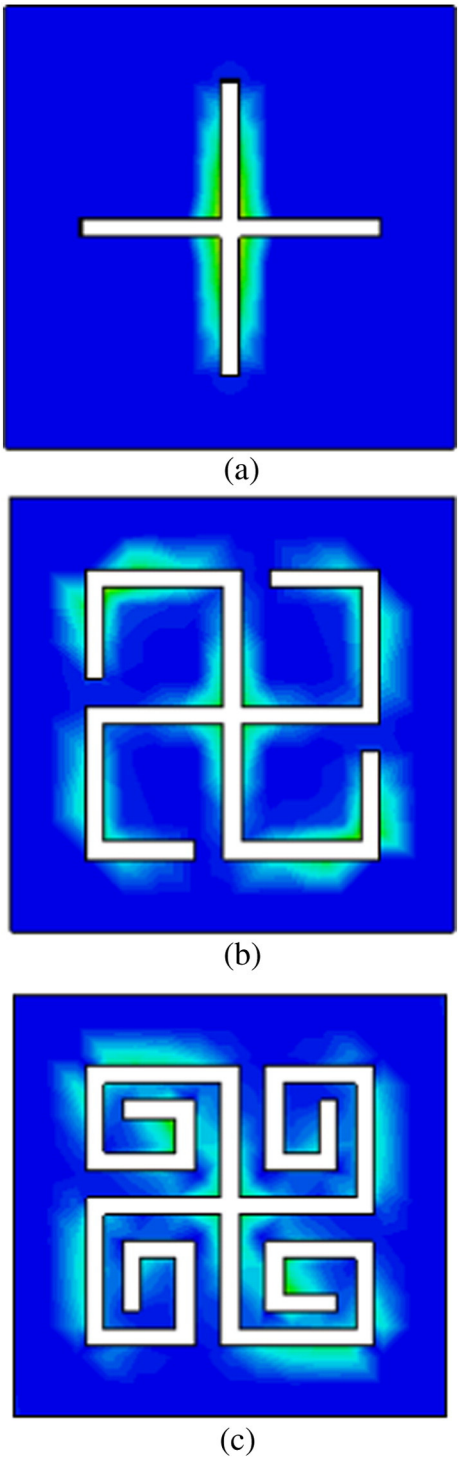

Fig. 5. The nano-antenna field intensity enhancement distribution for the main resonance (a) the simple nano-aperture (b) the L-shape nano-aperture (c) the novel cross nano-aperture.

Fig. 6(a) shows the effect of material loading on the nano-antenna resonance with Chemical potential of 0.1 eV. In this case, the peak resonances are reduced from 35.6 to 33.4 THz and 67.7 to 63.9 THz by increasing the refractive index of biomaterial respectively for first and second resonances. To continue, the result is checked for Chemical potential of 0.3 eV and as shown in Fig. 6(b) 40 to 37.5 THz and 70 to 66.4 THz by increasing the refractive index of biomaterial respectively for first and second resonances.

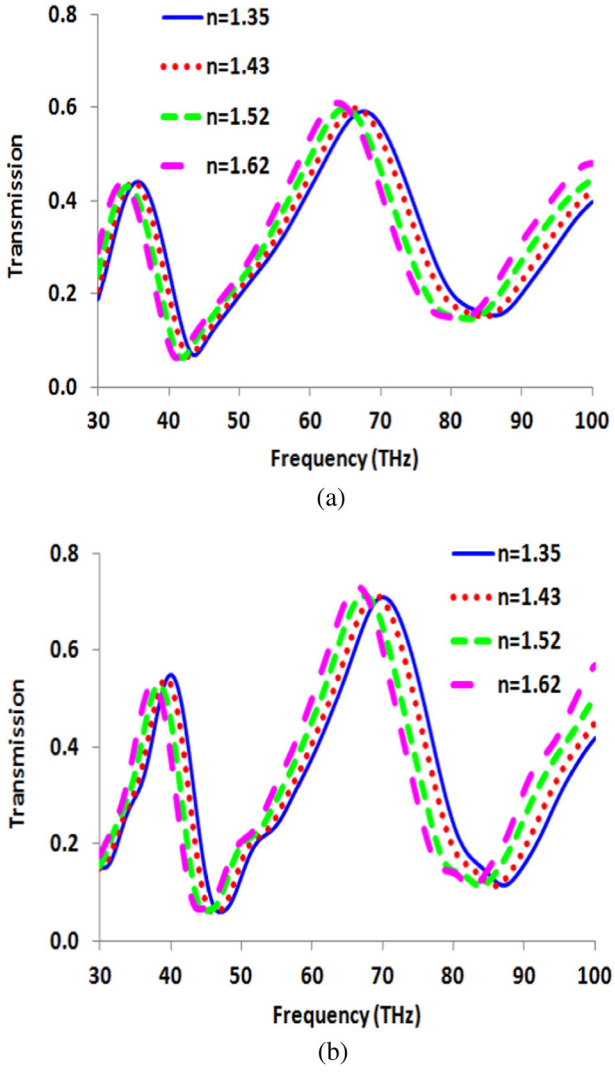

Fig. 6. Nano-aperture transmittance in presence of bio-chemical material (a) with graphene Chemical potential of 0.1 eV (b) with graphene Chemical potential of 0.3 eV.

Figure of merit (FOM) is a numerical factor for a description of the quality characteristic and performance of a device or a material for special parameter and in optical devices, various forms of FOM for wavelength (Δλ), current density (ΔI) and energy change (ΔE) [27–29]. Ahmadivand et al. have been debating about of (ΔE) variation by implementation of the biomaterial in plasmonic structure [27].

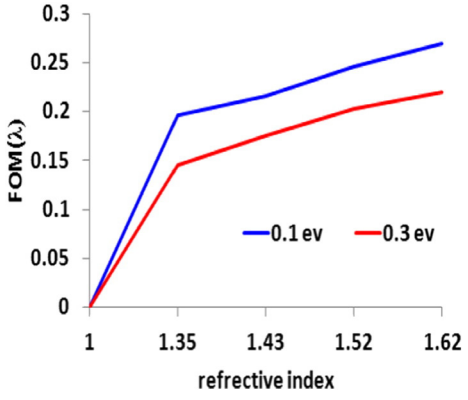

Fig. 7. The refractive index variations as a FOM profile for various biasing of the graphene at 0.1 and 0.3 eV.

As shown in Fig. 6(a) and (b) the wavelength (frequency) is shifted by applying the biomaterial this various in wavelength (Δλ) or energy (eV) can give us a factor for FOM.

In here, we are calculating the FOM of wavelength for two various amounts of the chemical potential of 0.1and 0.3 eV and results are presented at Fig. 7 second resonance at 70 THz (3696 nm). The FOM is reduced by increasing the chemical potential of the graphene layer to 0.3 eV. However, here we have two parameters for FOM and we can recognize the external material with more accuracy with logical operation on the result of the FOM.

In addition, the FOM results revealed that by increasing the graphene chemical potential, we have less tolerance by adding biochemical material load and the FOM result for nano-particle antenna is more in comparison to this study [27].

4. Conclusion

For making biosensor with nano-aperture, we presented new fractal shape with a single layer graphene coat and we show that the prototype structure is useful for achieving more sensitive and accurate sensor. Dual band characteristic at mid infrared is obtained. We show that at prototype structure by implementation of graphene layer we are able to achieved higher enhancement of E-field at prototype structure and FOM factor is controllable with graphene chemical potential.

References

[1] A. Nejati, R.A. Sadeghzadeh, F. Geran, Effect of photonic crystal and frequency selective surface implementation on gain enhancement in the microstrip patch antenna at terahertz frequency, Phys. B Condens. Matter 449 (2014) 113–120.

[2] Arif E. Cetin, Ahmet F. Coskun, Betty C. Galarreta, Min Huang, David Herman, Aydogan Ozcan, Hatice Altug, Handheld high-throughput plasmonic biosensor using computational on-chip imaging, Light: Science & Applications 3 (1) (2014), e122.

[3] X. Gao, L. Ning, Numerical study on plasmonic waveguiding effect of metallic nanorods structures, Optik-International Journal for Light and Electron Optics 124 (9) (2013) 828–831.

[4] Sergiy Steshenko, Filippo Capolino, Pekka Alitalo, Sergei Tretyakov, Effective model and investigation of the near-field enhancement and subwavelength imaging properties of multilayer arrays of plasmonic nanospheres, Phys. Rev. E 84 (1) (2011) 016607.

[5] Shan Huang, Zheyu Fang, Jie Li, Feng Lin, Xing Zhu, Plasmonic properties and device in nanostructures, Applied Physics A 112 (1) (2013) 15–22.

[6] P. Kvasnička, K. Chadt, M. Vala, M. Bocková, J. Homola, Toward single-molecule detection with sensors based on propagating surface plasmons, Opt. Lett. 37 (2) (2012) 163–165.

[7] Renming Liu, Deqing Zhang, Chenbo Cai, Xiong Yang, Sunce Li, Su Yongbo, Minzhen Si, NIR-SERS studies of DNA and DNA bases attached on polyvinyl alcohol (PVA) protected silver grass-like nanostructures, Vib. Spectrosc. 67 (2013) 71–79.

[8] Lijian Zhang, Fuchun Xi, Jie Xu, Qinbai Qian, Peng Gou, Zhenghua An, Strong light-matter coupling in plasmonic microcavities, Opt. Commun. 331 (2014) 128–132.

[9] Arif E. Cetin, Mustafa Turkmen, Serap Aksu, Dordaneh Etezadi, Hatice Altug, Multi-resonant compact nanoaperture with accessible large nearfields, Applied Physics B 118 (1) (2015) 29–38.

[10] Ekin Aslan, Sabri Kaya, Mustafa Turkmen, Enhanced transmission through periodic arrays of Jerusalem cross-shaped nanoapertures for sensing applications, Optical Sensors, Optical Society of America 2014, p. SeM2C-3.

[11] Mustafa Turkmen, Serap Aksu, A.E. Çetin, A. Ali Yanik, Hatice Altug, Multi-resonant metamaterials based on UT-shaped nano-aperture antennas, Opt. Express 19 (8) (2011) 7921–7928.

[12] R. Ning, S. Liu, H. Zhang, B. Bian, X. Kong, Tunable absorption in graphene-based hyperbolic metamaterials for mid-infrared range, Phys. B Condens. Matter 457 (2015) 144–148.

[13] Xingang Ren, Wei E.I. Sha, Wallace C.H. Choy, Tuning optical responses of metallic dipole nanoantenna using graphene, Opt. Express 21 (26) (2013) 31824–31829.

[14] Zhengren Zhang, Su Xiaopeng, Yuancheng Fan, Pengfei Yin, Liwei Zhang, Xi Shi, Dynamically tunable Fano resonance in planar structures based on periodically asymmetric graphene nanodisk pair, Phys. B Condens. Matter 473 (2015) 7–10.

[15] George W. Hanson, Dyadic Green's functions and guided surface waves for a surface conductivity model of graphene, J. Appl. Phys. 103 (6) (2008) 064302.

[16] Nima Dabidian, Iskandar Kholmanov, Alexander B. Khanikaev, Kaya Tatar, Simeon Trendafilov, S. Hossein Mousavi, Carl Magnuson, Rodney S. Ruoff, Gennady Shvets, Electrical switching of infrared light using graphene integration with plasmonic Fano resonant metasurfaces, ACS Photonics 2 (2) (2015) 216–227.

[17] Shou-En Zhu, G.C.A.M. Janssen, Optical transmittance of multilayer graphene, EPL (Europhys. Lett.) 108 (1) (2014) 17007.

[18] Marinko Jablan, Hrvoje Buljan, Marin Soljačić, Plasmonics in graphene at infrared frequencies, Phys. Rev. B 80 (24) (2009) 245435.

[19] Arif E. Cetin, Sabri Kaya, Alket Mertiri, Ekin Aslan, Shyamsunder Erramilli, Hatice Altug, Mustafa Turkmen, Dual-band plasmonic resonator based on Jerusalem cross-shaped nanoapertures, Photonics Nanostruct. Fundam. Appl. (2015).

[20] Arif E. Cetin, Mustafa Turkmen, Serap Aksu, Hatice Altug, Nanoparticle-based metamaterials as multiband plasmonic resonator antennas, IEEE Trans. Nanotechnol. 11 (1) (2012) 208–212.

[21] S. Sederberg, A.Y. Elezzabi, Sierpinski fractal plasmonic antenna: a fractal abstraction of the plasmonic bowtie antenna, Opt. Express 19 (11) (2011) 10456–10461.

[22] L. Rosa, K. Sun, S. Juodkazis, Sierpinski fractal plasmonic nanoantennas, Phys. Status Solidi RRL 5 (5–6) (2011) 175–177.

[23] G. Volpe, G. Volpe, R. Quidant, Fractal plasmonics: subdiffraction focusing and broadband spectral response by a Sierpinski nanocarpet, Opt. Express 19 (4) (2011) 3612–3618.

[24] L.H. Zhu, M.R. Shao, R.W. Peng, R.H. Fan, X.R. Huang, M. Wang, Broadband absorption and efficiency enhancement of an ultra-thin silicon solar cell with a plasmonic fractal, Opt. Express 21 (103) (2013) A313–A323.

[25] X. Huang, S. Xiao, D. Ye, J. Huangfu, Z. Wang, L. Ran, L. Zhou, Fractal plasmonic metamaterials for subwavelength imaging, Opt. Express 18 (10) (2010) 10377–10387.

[26] Fred Schedin, Elefterios Lidorikis, Antonio Lombardo, Vasyl G. Kravets, Andre K. Geim, Alexander N. Grigorenko, Kostya S. Novoselov, Andrea C. Ferrari, Surface-enhanced Raman spectroscopy of graphene, ACS Nano 4 (10) (2010) 5617–5626.

[27] Arash Ahmadivand, Raju Sinha, Nezih Pala, Hybridized plasmon resonant modes in molecular metallodielectric quad-triangles nanoantenna, Opt. Commun. 355 (2015) 103–108.

[28] Kenneth Diest, Vladimir Liberman, Donna M. Lennon, Paul B. Welander, Mordechai Rothschild, Aluminum plasmonics: optimization of plasmonic properties using liquid-prism-coupled ellipsometry, Opt. Express 21 (23) (2013) 28638–28650.

[29] Andreas Tittl, Christian Kremers, Jens Dorfmüller, Dmitry N. Chigrin, Harald Giessen, Spectral shifts in optical nanoantenna-enhanced hydrogen sensors, Opt. Mater. Express 2 (2) (2012) 111–118.